New Journal of Physics
The open-access journal for physics

Retention mechanisms and binding states of deuterium implanted into beryllium

M Reinelt[1], A Allouche[2], M Oberkofler[1] and Ch Linsmeier[1,3]

[1] Max-Planck-Institut für Plasmaphysik, EURATOM Association, Boltzmannstrasse 2, 85748 Garching b. München, Germany
[2] Physique des Interactions Ioniques et Moléculaires, CNRS and Université de Provence, Campus Scientifique de Saint Jérôme, Service 242, 13397 Marseille Cedex 20, France
E-mail: linsmeier@ipp.mpg.de

New Journal of Physics **11** (2009) 043023 (19pp)
Received 31 December 2008
Published 17 April 2009
Online at http://www.njp.org/
doi:10.1088/1367-2630/11/4/043023

Abstract. The retention of 1 keV D^+ ions implanted into clean and oxidized single crystalline Be at room and elevated temperatures is investigated by a combination of *in situ* analytical techniques including temperature programmed desorption (TPD), nuclear reaction analysis, low-energy ion spectroscopy (LEIS) and x-ray photoelectron spectroscopy. For the first time, the whole temperature regime for deuterium release and the influence of thin oxide films on the release processes are clarified. The cleaned and annealed Be sample has residual oxygen concentration equivalent to 0.2 monolayer (ML) BeO in the near-surface region as the only contamination. LEIS shows that Be from the volume covers thin BeO surface layers above an annealing temperature of 1000 K by segregation, forming a pure Be-terminated surface, which is stable at lower temperatures until again oxidized by residual gas. No deuterium is retained in the sample above 950 K. By analyzing TPD spectra, active retention mechanisms and six energetically different binding states are identified. Activation energies (E_A) for the release of D from binding states in Be are obtained by modelling the experimental data. Two ion-induced trap sites with release temperatures between 770 and 840 K ($E_A = 1.88$ and 2.05 eV, respectively) and two trap sites (release between 440 and 470 K) due to supersaturation of the bulk above the steady state fluence of 2×10^{17} cm^{-2} are identified. None of the release steps shows a surface recombination limit. A thin BeO surface layer introduces an

[3] Author to whom any correspondence should be addressed.

additional binding state with a release temperature of 680 K. Implantation at elevated temperatures (up to 530 K) changes the retention mechanism above the saturation limit and populates a binding state with a release temperature of 570 K.

Contents

1. Introduction

Currently, the material of choice for the plasma facing first wall of ITER's main chamber is beryllium (Be). Fuels for a fusion reactor are the heavy hydrogen isotopes deuterium (D) and tritium (T). Escaping energetic hydrogen isotopes from the plasma are implanted into the first wall materials. As Be will cover an area of almost 700 m^2, large amounts of tritium could be retained in the material or lost by permeation into structural components of the vessel. Increased temperatures can release implanted hydrogen again [1]. Reliable predictions of this recycling behaviour of the complete first wall require a detailed understanding of the interactions of hydrogen and Be. Although much experimental data have been acquired in the past [2]–[6], the details of the processes that influence the recycling are still unclear. This can be seen particularly in the widely differing values of hydrogen isotope retention and release (diffusivity, solubility, detrapping energies, etc) [7]. Three possible reasons for the disagreeing results are considered:

Firstly, unknown chemical compositions of the samples, especially oxidized surfaces, can influence thermally activated release processes. Desorbing gaseous species have to pass the surface and, especially in the case of hydrogen, must recombine to molecules (within the expected relevant temperature range) in order to desorb. The release rate can therefore be limited by surface processes. Even a closed monolayer (ML) impurity coverage can thereby introduce an energetic barrier to recombination. The surface of Be is quickly covered by a closed beryllium oxide (BeO) layer [8] introducing a factor of uncertainty to the analysis of experimental retention data. According to the results from Zalkind *et al* [8], BeO grows quickly initially from the gas phase in the form of islands, which leads to a closed BeO surface at a coverage of 3 ML (after exposure to only tens of Langmuirs), when the growth mechanism changes and the rate slows down. The fast growth rate at sub-ML coverages makes experiments with clean Be surfaces technically very demanding, even under good UHV conditions.

Secondly, hydrogen transport in Be is influenced by the substrate structure. The crystalline configuration is especially of importance, because diffusivities through an undisturbed lattice

and along grain boundaries can differ significantly. Before hydrogen exposure, an unknown density and character of defects in the Be lattice can constitute possible trap sites for hydrogen, introducing an additional factor of uncertainty to models and simulation.

Finally, in order to obtain characteristic values describing the hydrogen recycling, the retention mechanisms must be identified to apply the appropriate modelling, from which quantitative activation barriers for hydrogen release are determined.

Due to these considerations, this work places special emphasis on the structure and the chemical composition of the substrate and the identification of the retention mechanisms in the experiments.

One way to obtain characteristic values, especially activation energies, is to model the temperature- and therefore energy-dependent release of implanted hydrogen. By heating an implanted Be sample in a controlled, preferably linear manner (temperature programmed desorption, TPD), spectra of hydrogen desorption rate versus time, and therefore temperature, can be measured. Unlike the desorption of adsorbed molecules from a surface, the release of implanted gaseous species from within a bulk material is influenced by a combination of bulk- and surface-controlled processes. By minimizing the experimental uncertainties in surface composition and sample structure, single processes can be separated and identified. We discuss the experimental results from a phenomenological point of view to derive the retention mechanisms and the processes that govern the temperature-dependent release of implanted D. The qualitative models are then cast into quantitative TMAP7 [9] modelling and rate equations in order to obtain activation energies from the experimental TPD data. Density functional theory (DFT) calculations of the structural evolution of the Be lattice and hydrogen-bonding upon increasing D concentration allow further insights. The binding energies obtained from these calculations, which directly picture the system after implantation, are related to the activation energies obtained from the modelling of the release processes. This provides the possibility of drawing conclusions about the retention mechanism itself.

2. Experimental procedure

The Be sample under investigation is a single crystalline disc of 0.4 mm thickness and 14 mm in diameter. The single crystallinity was confirmed by Laue diffractography and shows an orientation of the mirror-polished surface of $(11\bar{2}0)$ with a deviation of less than 1°. The surface of the Be sample was cleaned under UHV conditions by numerous cycles of bombardment with 3 keV Ar^+ ions under 45° incident angle at room temperature and underwent subsequent annealing up to 1000 K. The chemical surface composition is monitored by x-ray photoelectron spectroscopy (XPS) and low-energy ion spectroscopy (LEIS). The LEIS spectra are recorded with a 480 eV He ion beam under an angle of incidence of 45°. XPS measurements are performed with a non-monochromatic x-ray source with Mg Kα radiation. For both analytical techniques a hemispherical analyzer (model PHI 10-360) is used. A minimal residual oxide coverage of 0.2 ML on the annealed sample as the only contamination is achieved and maintained for several hours at a base pressure of 2×10^{-11} mbar in the vacuum chamber. The sample is thoroughly degassed, so that during annealing up to 1000 K, the pressure in the chamber does not rise above 1×10^{-9} mbar and thus no additional oxygen uptake on the sample surface is observed by XPS. Higher oxygen coverages (up to 3 ML) are obtained by storing the sample under UHV conditions for more than 24 h, allowing a BeO layer to grow

from the residual gas. The sample is prepared as described and bombarded by a mass-separated, monoenergetic 3 keV D_3^+ ion beam incident perpendicular to the surface. This molecular kinetic energy corresponds to a kinetic energy of 1 keV per D atom. The beam profile and irradiation fluence are measured using a Faraday cup with a pinhole opening of 0.5 mm diameter. As far as it is detectable by XPS, the chemical composition of the cleaned sample surface does not change with implantation. TPD experiments are performed by heating the sample with a linear rate from the back via electron impact. The surface temperature is measured by an Ni/CrNi thermocouple spot welded to the sample surface. Pre-programmed and optimized temperature ramps of 0.5, 1.0 and 4.0 $K\,s^{-1}$ are used. The released gas flux is detected by a differentially pumped quadrupole mass spectrometer (modified Balzers QMG 422) in line-of-sight geometry. The desorbing deuterium flux is calibrated by measuring the retained deuterium areal density after implantation *in situ* by nuclear reaction analysis (NRA). Details are given in Reinelt and Linsmeier [10]. The reaction $D(He^3, p)^4He$ with 800 keV $^3He^+$ ions from a 3 MV tandem accelerator is used [11]. The integrated TPD flux is set equal to the measured areal density by NRA. After a TPD experiment up to 1000 K, no residual D can be detected in the sample either by NRA or by successive TPD runs. The complete experimental set-up is described elsewhere in detail [12].

3. Results and discussion

3.1. Sample surface characterization

To gain information on the evolution of the surface composition during the temperature treatments, LEIS spectra are recorded at different substrate temperatures to show the composition of the first ML of the sample. For this experiment, the sample surface is covered by a closed, 3 ML thick BeO layer grown from the residual gas during 24 h. Figure 1 shows the corresponding LEIS and XPS O 1s spectra after flash heating the sample to the denoted temperature. After switching off heating, LEIS and XPS spectra are recorded during cooling down. At temperatures below 1005 K, LEIS shows a clear peak at $0.36E/E_0$, which is assigned to oxygen. The indication of a shoulder at $0.17E/E_0$, almost covered by the background of secondary ions, is assigned to Be. The relative Be and O intensities reflect qualitatively the composition of the first ML of the sample. The corresponding O 1s binding energy region measured by XPS is shown in the right panel of figure 1. In contrast to LEIS, XPS probes not only the first atomic layer, but a surface region up to a depth of several nm. After heating the sample to temperatures above 875 K, LEIS and XPS spectra show different compositions of the sample's first layer (LEIS) and the near-surface region (XPS). The oxygen in the first ML vanishes and a clear peak at $0.17E/E_0$ indicates a Be-terminated surface. Simultaneously, the intensity of the O 1s peak in the XPS spectra decreases and exhibits a shift of 0.8 eV to higher binding energies. These observations are explained by segregation of metallic Be from the bulk through the BeO surface layer above 875 K, taking into account that BeO cannot evaporate at this temperature (melting point $T_M(\mathrm{BeO}) = 2851$ K). The metal-terminated surface is stable at lower temperatures, until again oxidized by oxygen or water from the residual gas. The decrease of the O 1s intensity in the XPS spectra is caused by the covering of the outermost oxygen, attenuating the photoelectron intensity and changing the chemical state of the surface oxygen atoms. The shift in the binding energy of the total O 1s peak can therefore be explained by assuming that the total O 1s peak is composed of two oxygen species with different O 1s binding

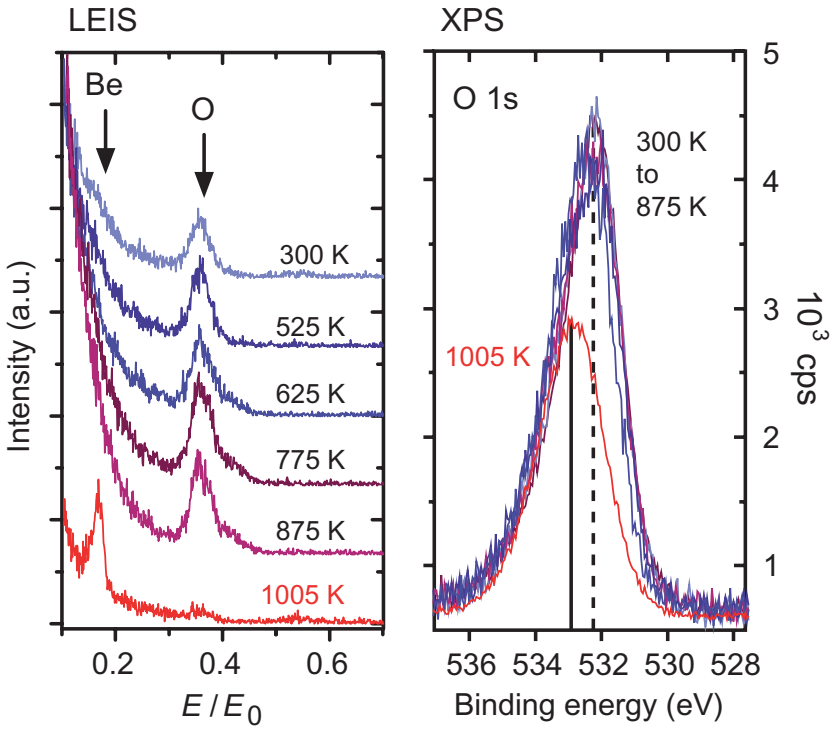

Figure 1. LEIS (left) and XPS (right) spectra of a BeO-covered (3 ML) Be sample, flash heated sequentially to the indicated temperatures. Above 875 K, Be from the bulk segregates towards the surface, burying the oxide layer. The photoelectron intensity of the O 1s core levels is attenuated by this overlayer. The shift in the binding energy indicates two oxygen-binding states (vertical lines), one associated with oxygen at the surface (dashed line).

energies. The binding energy of the species corresponding to surface oxygen is shifted towards higher binding energy when covered with beryllium. This interpretation is in agreement with the previous observation in ^{18}O marker experiments [13] investigating the growth mechanism of BeO. The conclusion of these observations is the onset of Be diffusivity at about 900 K, clearly below the bulk melting temperature of Be metal, $T_M(\mathrm{Be}) = 1551$ K.

Ex situ SEM images of the single crystal surface without any treatment by ion bombardment, but several heating cycles up to 100 K, show the formation of large crystallite structures (up to 100 μm) with uniform geometry and alignment across the sample surface. The 30° tilted surfaces of the crystallite facets have a $(10\bar{1}0)$ orientation. The front facet of the crystallites shows the (0001) surface, as indicated in figure 2(a). According to the conclusions from the LEIS and XPS measurements, the crystallites are formed by a recrystallization process to lower indexed surfaces when the sample is heated up to 1000 K, driven by the reduction of surface energies for low-indexed facets. The size of the structures indicates a considerable mass transport. From these observations, we conclude that after cleaning and annealing up to 1000 K, the sample surface region is structurally and chemically well defined with a Be-terminated surface, that defects due to ion bombardment are annealed and that the sample is in a single crystalline state.

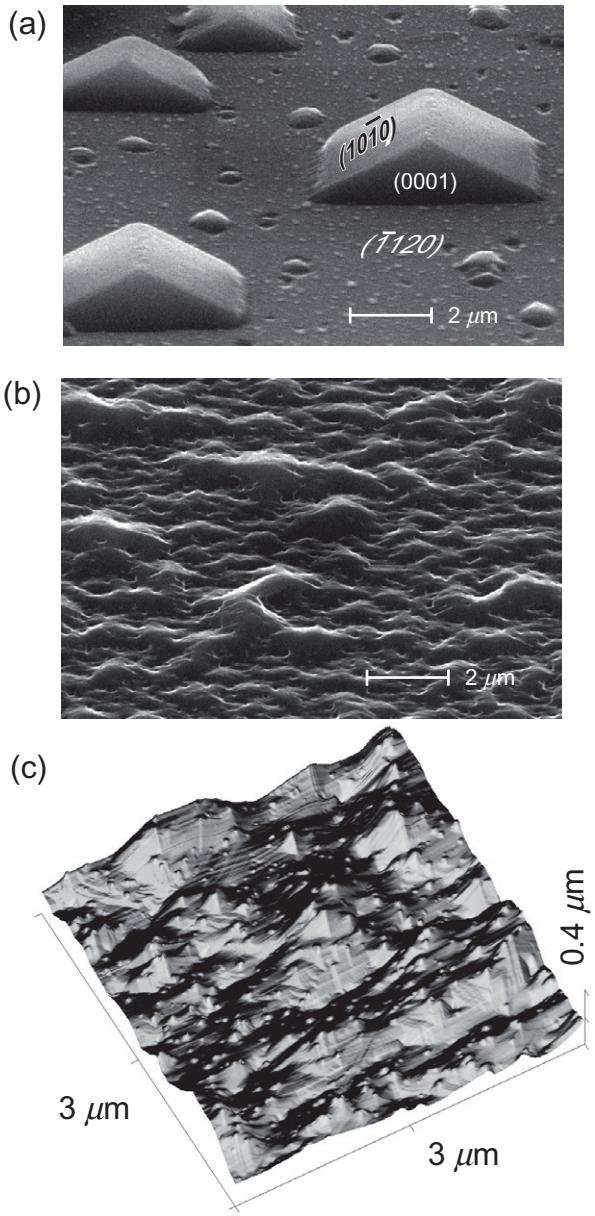

Figure 2. SEM images of the (a) cyclically annealed (1000 K) and (b) annealed, D irradiated and degassed single crystalline Be surface. Recrystallization forms large crystallites with lower surface energies. D sputtering competes against recrystallization and forms structural modifications. Their morphology can be seen as nm-sized protrusions in the AFM image in (c).

After several D^+ irradiations, TPD experiments and cleaning cycles, the sample surface exhibits a heavily modified microscopic structure, as shown in the SEM image in figure 2(b). However, a large part of the roughness is caused by the recrystallization process described above, as there is a clear transition from well-shaped crystallites to rough and eroded structures along the sample surface. This lateral transition of the surface morphology is related to the locally applied ion fluence (Ar and D bombardment). Small protrusions (up to 100 nm in

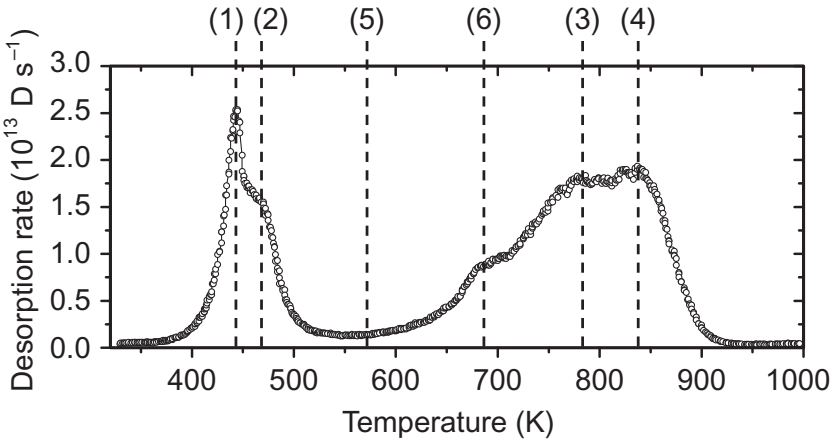

Figure 3. TPD spectrum of $m/q = 4(D_2)$, acquired with a heating rate of $1\,K\,s^{-1}$, measured after an incident D fluence of $2 \times 10^{17}\,cm^{-2}$, implanted at room temperature into an annealed single crystalline Be sample. The sequential release occurs at six different temperatures indicating six energetically different activation energies.

diameter) can be found on the D irradiated surface. Although these modifications appear as small holes in the SEM image in figure 2(b), their real morphology is revealed by atomic force microscopy (AFM). AFM imaging (figure 2(c)) in contact mode shows the topography of the microfacetted and partially recrystallized surface, which is covered with D-induced protrusions. The nature of these modifications will be discussed below.

3.2. Retention mechanisms

3.2.1. Implantation at room temperature. A typical TPD spectrum (figure 3) of $m/q = 4(D_2)$ with a heating rate of $1\,K\,s^{-1}$ after an incident D fluence of $2 \times 10^{17}\,cm^{-2}$, implanted at room temperature, shows a sequential release of D in two temperature regions. The contribution of HD to the overall deuterium release ($m/q = 3$) is two orders of magnitude lower due to the low H_2 background pressure in the chamber and shows mainly a peak at 470 K, which is omitted in the further discussions. A release of other species (D_2O, HDO, etc) was not observed. No background is subtracted from the spectra, because the rate drops quickly to the initial background pressure after complete desorption (above 950 K). The release peak at low temperatures (400–500 K) is composed of two distinct peaks: peak (1) at a temperature of 440 K and peak (2) at 470 K. Release of deuterium in this temperature region was previously reported by Markin *et al* [14]. A broad release feature at high temperature is composed of peak (3) at 770 K and peak (4) at 840 K. A shoulder at a temperature of 680 K indicates an additional peak (6). Between the main peaks (1, 2) and (3, 4), an increased background (5) hints at additional release peaks with low occupation. To model this experimental spectrum, the nature of the rate-limiting step for each of the release peaks (1)–(6) has to be identified.

A lateral analysis of the irradiation spot with NRA shows a deuterium distribution in the form of the lateral ion implantation profile. This means that D is retained locally at its implantation position and does not diffuse or dissolve in the Be bulk. TPD spectra with increasing incident fluence exhibit a sequential occupation of the binding states (figure 4) from

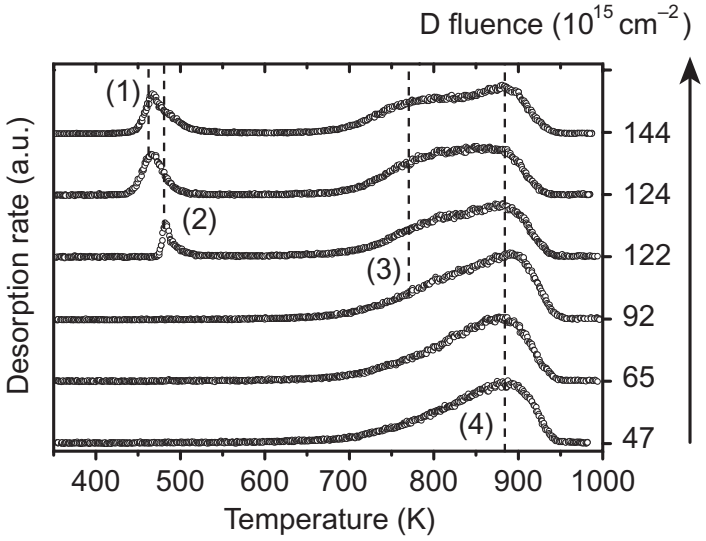

Figure 4. Series of TPD spectra with varying incident deuterium fluences implanted at room temperature. The release states are occupied sequentially from (4) to (1), indicating local saturation of the binding sites. States (1) and (2) show a threshold behaviour. The spectra are measured at random fluence steps.

higher (state 4) to lower release temperatures (state 1). This behaviour can be explained by a saturation of the available binding sites, as lower release temperatures indicate lower activation energies and therefore energetically unfavourable sites. The ratio of occupation of states (3) and (4) changes with increasing fluence. A constant retention of $78 \pm 5\%$ is measured up to an incident fluence of 1×10^{17} cm^{-2}.

Based upon the conclusions from the sample characterization, the Be lattice is in an undisturbed and single crystalline state when, at very low irradiation fluences, the first hydrogen atoms are implanted. Due to the collision cascades initiated by the impinging D ions, defects are created in the lattice which can act as trap sites with a higher binding energy for hydrogen. At the end of the atom trajectories (where most of their kinetic energy is dissipated by collisions) D is not necessarily bound to such a high-energy trap (state 3 or 4), but can diffuse freely through the bulk, until trapped by one of these two types of trap sites. This retention mechanism explains why the ratio of occupation changes with increasing fluence. This description also agrees with an apparently fast diffusivity at room temperature [15]. Gas-loaded Be samples examined by Macaulay-Newcombe *et al* [16] also show a release in two peaks at temperatures similar to those of peaks (3) and (4) observed in this work. The amount and ratio of occupation depends on the fabrication method of the Be samples. Neutron-irradiated samples show a release of hydrogen starting at a temperature of at least 775 K [17], above the temperature of peak (3). These observations support the assignment of release peaks (3) and (4) to detrapping from defects in the lattice, which are created by the collision cascade due to D implantation. These types of trap sites can also be intrinsically present in materials, depending on the structure, or can be created by neutron irradiation.

In contrast to the release from high-energy traps, the release from low-temperature states (1) and (2) shows a threshold behaviour as a function of implantation fluence. Above a fluence of 1×10^{17} cm^{-2}, initially state (2) is occupied and at higher fluences, predominantly state (1) is

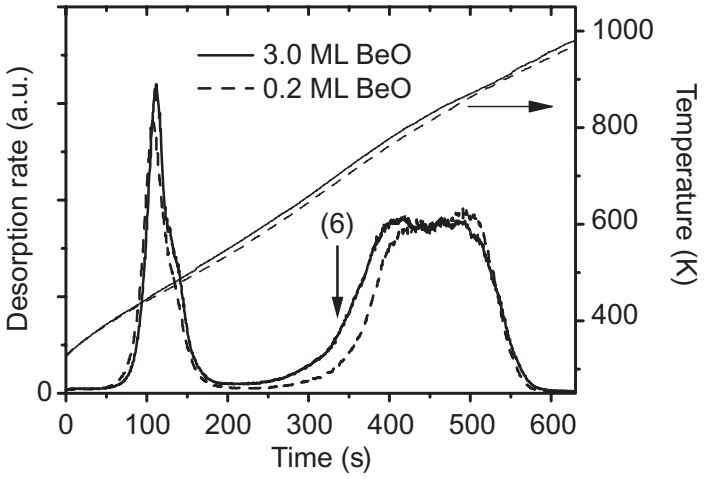

Figure 5. TPD spectra of cleaned (0.2 ML residual oxygen coverage) Be and release via a closed BeO-covered surface (3 ML). None of the release peaks is influenced by changing the surface composition and, thus, the processes are not recombination limited. State (6) shows a slightly increased occupation, indicating the decomposition of a surface hydroxide.

occupied. The spectrum series in figure 4 was recorded in random order after intermittent sample preparation to prevent the influence of sample history. Implantation of fluences lower than 1×10^{17} cm^{-2} does not lead to the formation of states (1) and (2). It is therefore concluded that these states are created due to a deuterium concentration build-up in the sample. Although the release temperatures of (1) and (2) are similar to desorption from a surface, the amount originating from these states is 60 times the saturation coverage of a Be surface with D [18], which cannot be explained by surface roughness alone. AFM measurements (figure 2(c)) indicate a surface roughness, which increases the (flat) projected surface area by not more than a factor of 1.2. Therefore, surface desorption processes from adsorbed D as rate limiting processes are excluded here. The released D_2 originates from D retained in the collision-cascade-modified Be lattice.

3.2.2. Influence of a BeO-covered surface. Under normal operation conditions in ITER, the Be first wall will be covered by various compound surface layers, one of them being BeO. As already pointed out, even one closed ML of a different material on a Be surface could represent an energy barrier for the recombination process of hydrogen, altering the release parameters. To investigate this issue, a TPD spectrum is recorded in the described manner with an incident D fluence of 2×10^{17} cm^{-2} and a BeO coverage of 0.2 ML. For a second experiment, the cleaned and annealed Be is implanted with the same incident fluence. In this experiment, however, after loading the substrate with D, a 3 ML closed BeO surface layer is allowed to grow from the residual gas in the UHV chamber. The segregation of Be bulk material to form the Be-terminated surface takes place above 900 K, which means that desorption in a TPD experiment with this sample preparation must occur via a completely BeO-covered surface. Both TPD spectra (shown in figure 5) are recorded with the same temperature ramp of 1 K s^{-1}. Any difference in the two spectra obtained by the two experiments can hence be directly related to the influence of the thin

BeO layer. If one of the observed release states (1)–(4) were rate limited by a surface process (such as recombination), a change of the surface composition from Be to BeO would shift the corresponding activation energy for this surface process (e.g. surface diffusivity). This would then alter the measured peak temperature. However, none of the binding states (1)–(4) is shifted or changed significantly. Instead, for the sample with 3 ML BeO a slightly increased amount of D is bound in state (6), indicated by an arrow in figure 5. A release of D in the form of D_2O or HDO is not observed. Three conclusions can be drawn from this experiment. Firstly, the retention is not significantly influenced by a thin 3 ML BeO coverage on the surface. This is to be expected for the discussed retention mechanisms in the Be bulk. Secondly, none of the peaks is shifted in its temperature, which would be expected if any of the states were limited by a surface process. From this it can be concluded that the activation energy for the reaction $2D \rightarrow D_2$ on Be and BeO surfaces is lower than the barriers for the release processes observed in these experiments. In TDS experiments [18], desorption of (chemisorbed) D from a clean Be surface was seen to start at 400 K, whereas from an oxidized surface, desorption was observed already at 300 K. Thirdly, release peak (6) is related to the BeO-covered surface. It stands to reason that D is bound as BeO–D at the surface and that decomposition of this surface hydroxide (to BeO and D_2) leads to release peak (6). TPD spectra of oxidized Be samples [4] show an increased release at about 700 K, the temperature region of release peak (6).

3.2.3. Retention of deuterium. A major issue in plasma–wall interaction in fusion reactors is the retention behaviour of the first wall materials. The retention behaviour is the basis for estimating fuel recycling and safety limits regarding tritium accumulation. From integration of calibrated TPD fluxes, the retention of D implanted into clean Be at room temperature can be obtained. Figure 6(a) shows the measured retained deuterium areal density (circles) as a function of deuterium irradiation fluence. Each circle represents the retained D fluence from one integrated TPD experiment, performed after preparation of a clean Be surface. At a fluence of 2×10^{17} cm^{-2}, the deuterium retention in the sample reaches a steady state. This value is in good agreement with previous studies [7, 19]. Below the steady state fluence, the retention (retained areal density/incident fluence) is $78 \pm 5\%$, obtained from a linear fit to the data points (not shown). Figure 6(c) shows D depth profiles of a dynamic SDTrim.SP calculation (a Monte Carlo code simulating the kinematic interactions of a particle impinging on a solid target based on the binary collision approximation [20, 21]), in which accumulation of D in the Be matrix by implantation is allowed. The profiles show that the concentration build-up by implantation in the bulk is faster than the loss of D by sputtering. This leads to a local concentration of 20–25 at% deuterium in a depth of 40 nm in the Be bulk at an incident fluence of 1×10^{17} cm^{-2}. The experimentally determined fraction of retained deuterium released from states (1) and (2) in figure 6(b) shows that this is the threshold fluence for creation of binding states (1) and (2). At this implantation fluence (and therefore local D concentration of 20–25 at% in the bulk), the Be bulk reaches local saturation, i.e. all locally available ion-induced defects are occupied. Additional implanted deuterium leads to the creation of binding states (1) and (2), which exhibit a lower release temperature. This means that the states are created due to local supersaturation of the bulk. Because the resulting structural modifications (also seen in the AFM image in figure 2(c) as small protrusions) cannot be accounted for by SDTrim.SP, the local concentration is limited to 0.26 at% deuterium in the simulation. The sample saturation is reached at higher fluences ($>2 \times 10^{17}$ cm^{-2}). The maximum local concentration of $D/Be = 0.35$ is also in good agreement with the literature values [7]. Because the concentration in the SDTrim.SP calculation

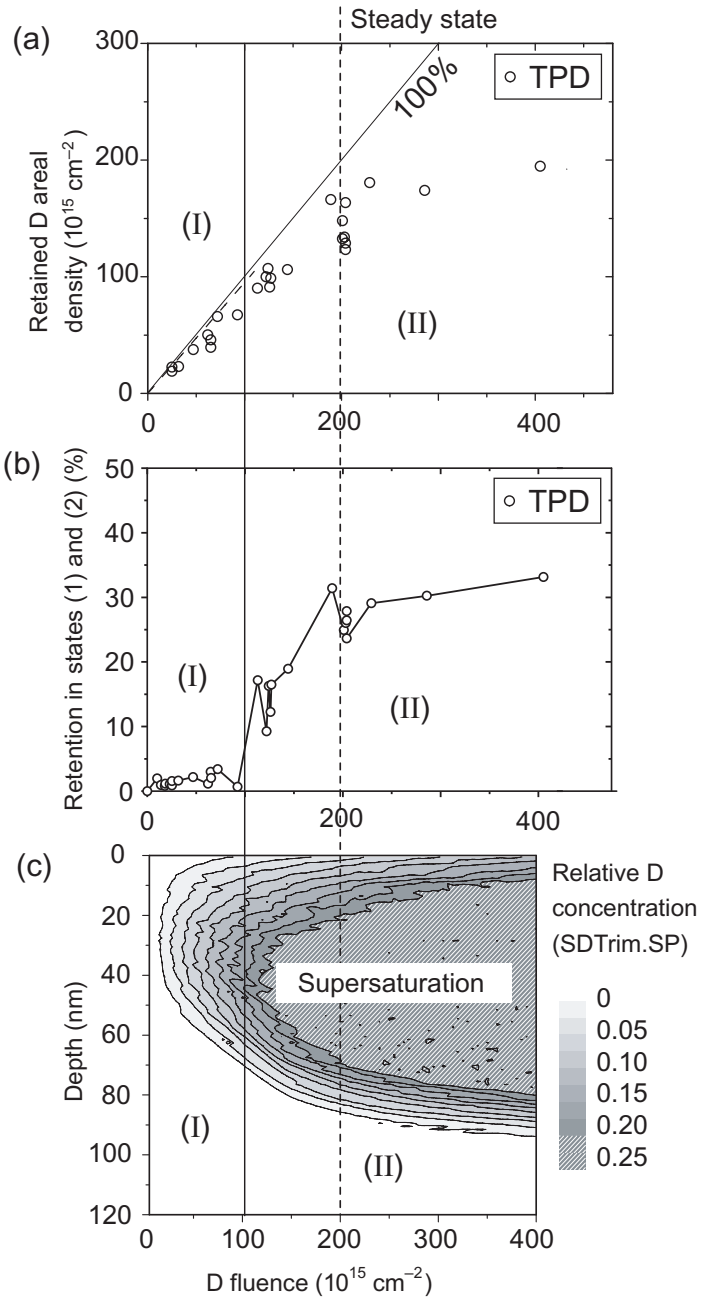

Figure 6. (a) Experimentally measured (by TPD) retained D areal density as a function of incident fluence. The fraction of deuterium retained in binding states (1) and (2) is illustrated in (b), showing a threshold behaviour. The experimental result is compared with a dynamic SDTrim.SP [21] calculation (c), which allows the accumulation of D in Be up to a local concentration of 0.26. This value is reached at a depth of 40 nm, as illustrated by the calculated concentration depth profiles (c) at an irradiation fluence just above 1×10^{17} cm^{-2}. The SDTrim.SP calculation is only valid in the fluence region denoted by (I). In region (II), states (1) and (2) appear in TPD spectra due to local supersaturation.

is clipped at this value, ignoring all additionally stopped D at this depth, the calculation is only valid below an incident fluence of 1×10^{17} cm^{-2} (denoted by region (I)). Region (II) indicates a supersaturated and structurally modified Be bulk.

According to transmission electron microscopy (TEM) imaging performed by Chernikov *et al* [22], nanostructural modifications in the form of cavities (diameter below 1 nm) appear in the Be lattice in the fluence region below 1×10^{17} cm^{-2}. It was deduced from TEM and secondary ion mass spectrometry (SIMS) experiments that D is present in the form of molecular deuterium (D_2) in closed cavities above the saturation limit. The D_2 pressure in the cavities was calculated to be in the range of GPa. However, if the assignment of the structural modifications to binding states (1) and (2) is correct, the release temperature of 470 K does not allow molecular D_2 to reabsorb as D into the Be bulk by dissociation. This step, however, is required for the diffusion to the sample surface and subsequent release into the vacuum. This step would consequently be rate-limiting requiring an activation energy above 2 eV per D atom (breaking of the D–D bond). Molecular deuterium does not chemisorb on Be [18], so the re-adsorption of D_2 from gas-filled bubbles into the Be lattice is not possible at 470 K. The release temperatures of (1) and (2) are also too low for a release mechanism involving crack formation in the bulk material due to a pressure increase. Because of the size of the structural modifications and the concentration in the supersaturated regions at fluences slightly above 2×10^{17} cm^{-2}, we conclude that the actual equilibrium concentration of molecular D_2 in the supersaturated regions must be close to zero. Deuterium is probably present in the form of a 'destabilized Be/D amorphous material', in which D is bound in a form energetically related to the adsorbed state on a surface. This explains the similarity of the release temperatures for states (1) and (2) and desorption from a Be surface. The temperature-dependent release process starts for both cases from a similar binding state of D to Be. For adsorbed deuterium on the sample surface, the release proceeds towards D_2 and desorption into vacuum. The release from the supersaturated regions (states 1 and 2) corresponds to a release of atomic deuterium into a solute (mobile) state in the Be bulk. The appearance of D_2 in SIMS and cavities in TEM [22] might be due to interference of the (destructive) analytical methods with the actual retention condition described above. Release of pressure from the system by sputtering during SIMS or thinning for TEM can, as a consequence, lead to the appearance of D_2 gas-filled cavities. Applying much higher fluences than performed in the experiments described here leads to the formation of a porous open network structure with channels of micrometre radius [23], although the maximum retention does not change significantly. High fluences relate to increasing damage and disordering of the material. The consequence is a restructuring of the (at first nanosized) supersaturated regions by aggregation to big cavities and channels, which are then filled with D_2 gas or are open to the vacuum.

3.2.4. Implantation at elevated temperatures. Implantation at elevated substrate temperatures is a common situation for plasma–wall interaction in a fusion experiment, as radiation and high particle fluxes impose a massive heat load on the material. At temperatures above 480 K, which is the expected normal operation temperature of the ITER Be first wall [1], binding states (1) and (2) cannot be occupied. Based on the previous discussion, one would expect that all implanted D is retained in binding states (3) and (4) and therefore released above 700 K. Instead, a TPD spectrum at an implantation temperature of 530 K shows that increased amounts of D are released from states (5) and (6), as shown in figure 7. This spectrum is directly compared with an experiment with implantation of the same deuterium

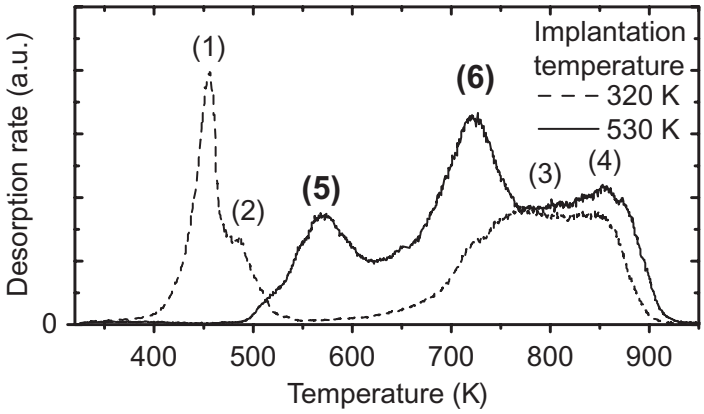

Figure 7. TPD spectra of D implanted into Be at temperatures of 320 and 530 K. Retention in the ion-induced trap sites (3) and (4) is not affected. The low-temperature binding states (1) and (2) are not occupied in the 530 K implantation experiment. Instead, increased amounts of D are retained in states (5) and (6).

fluence (2×10^{17} cm^{-2}) at 320 K. The condition of the substrates with respect to structure and chemical composition is identical for both experiments. The retention in states (3) and (4) seems to be unaffected, which is to be expected, if these peaks are governed by release from trap sites in the bulk. From this comparison, it can be concluded that the retention mechanism for an implantation fluence above the bulk saturation changes with an increase in implantation temperature. Binding state (5) is only noticeable as an increased background in room temperature implantation experiments. A hint about the nature of binding state (5) can be found in Barry *et al* [24] where the dissociation of beryllium hydride was investigated. Several investigations report a decomposition temperature of beryllium hydride, BeH_2, from 500 to 600 K, the peak temperature of state (5) [24]–[26]. Although no direct experimental data for BeD_2 are available, it can be assumed that the decomposition temperatures of BeH_2 and BeD_2 are similar. An elevated substrate temperature during implantation can allow a phase transition above the fluence threshold for the appearance of binding states (1) and (2) from a supersaturated Be lattice to BeD_2. However, this can only occur within a narrow temperature range, as the deuteride starts to decompose above 500 K. This explains why the occupation of state (5) is temperature dependent. Also during the run of a TPD experiment (after RT implantation), the elevated temperatures allow only small amounts of BeD_2 to be formed, as the majority of D from the supersaturated states, binding states (1) and (2), is already released at the formation temperature. During implantation at elevated substrate temperatures, most of the locally retained fluence above bulk saturation is retained as BeD_2. In this case, the hydride phase is formed during implantation. This also explains why in many experiments reported in [7], retention is rather constant up to an implantation temperature of 700 K, when finally occupation of states (5) and (6) is no longer possible. A persistent background at a temperature above 500 K is also observed in TDS experiments of adsorbed D atoms on a clean Be surface [18]. In [18], this was attributed to absorption of D in subsurface sites. In light of the present conclusions, this background is explained by a phase transformation of adsorbed D to BeD_2 during the desorption experiment, followed by subsequent decomposition of BeD_2 and release of D_2.

Increased amounts of deuterium are also released from state (6), assigned in the discussion above to release from an oxidized Be surface. Although the surface composition in the

irradiation spot does not show an increased BeO coverage, as measured by XPS, a higher diffusivity of D might allow D to reach uncleaned (BeO-covered) sample regions and form hydroxides, which can explain the increased amounts of D bound in state (6).

3.3. Modelling

3.3.1. Modelling of deuterium release. As a consequence of the qualitative assignment of the release peaks observed by TPD to retention mechanisms and binding states of D in Be, the spectra can be modelled using hydrogen transport and trapping codes. TMAP7 [9, 27] includes treatment of temperature transport, diffusion, surface recombination and trapping and is thus applicable for modelling the release from the ion-induced defects in release peaks (3) and (4). The code numerically solves the diffusion equation and applies flux equilibria as boundary conditions. The diffusivity is included as

$$\mathrm{D}(T) = 6.7 \times 10^{-9}\ \exp\left(\frac{-0.29\,\mathrm{eV}}{kT}\right) \tag{1}$$

from permeation experiments by Abramov *et al* [15]. The recombination on the clean surface follows the values given in [18] with an activation energy of desorption of 0.87 eV. Two types of trap sites in the bulk are used in the model, corresponding to release peaks (3) and (4). The trap concentration profiles are determined by the implantation collision cascades and therefore taken from implantation profiles calculated by static SDTrim.SP. For the TMAP7 simulation, these profiles are approximated by Gaussian-shaped distributions due to insignificant deviations in the calculation. All trap sites are filled with D at the beginning of the temperature ramp. The number of traps and therefore the overall retained amount of deuterium is taken from the experiment. The temperature is varied linearly according to the respective experiment. Desorption occurs via recombination into a vacuum volume with a constant partial pressure of 10^{-10} mbar (re-adsorption is negligible). The flux from the sample surfaces (front and back) is assumed to correspond to the TPD spectrum. The calculation shows that the flux contribution from the back of the sample is 5 orders of magnitude lower and thus negligible. A manual adjustment of the simulated flux to the TPD experiment by varying the activation energy for detrapping in the model yields activation energies of 1.88 eV for the release from trap site (3) and 2.05 eV for site (4). The model shows good agreement for different temperature ramps (0.5–4 K s^{-1}) and different incident fluences below 1×10^{17} cm^{-2}. Results of the TMAP7 simulation are shown in figure 8(a), together with the experimental data for D^+ implanted into clean Be at room temperature.

For the release peaks (1) and (2), TMAP7 cannot be used because dynamic changes of the substrate (i.e. structural modifications by supersaturation as discussed above) are not implemented in the code. For the release from this region of the TPD spectrum (350–550 K), a simple model is applied, which is based on rate equations [28] in the form of

$$R(T, N) = -\frac{\partial N}{\partial T}\frac{\partial T}{\partial t} = N^r \nu\ \exp\left(-\frac{E_\mathrm{A}}{kT}\right). \tag{2}$$

Several assumptions must be considered. First, the release rate R is determined by one rate-limiting step. Furthermore, this step must be temperature dependent and described by equation (2), where $\nu \approx 10^{13}\,\mathrm{s}^{-1}$ is a frequency factor, r the reaction order ($r = 1$ for this case) and E_A the activation energy of the release process. N is the deuterium amount in the

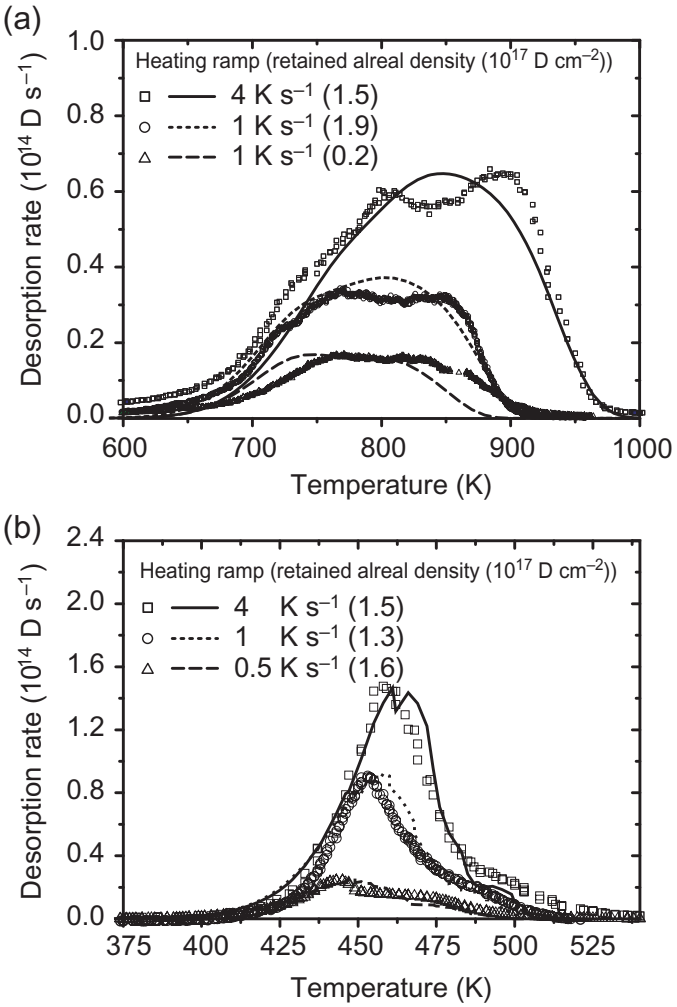

Figure 8. Experimental and simulated TPD spectra for D^+ implantation into clean Be at room temperature. (a) Comparison of simulated D release rates (TMAP7 model) from the ion-induced trap sites with experimental TPD spectra measured with varying D implantation fluence and heating rates. The differences in the peak temperatures between experiment and simulation are due to deviations of the temperature ramps. (b) Measured release rates from supersaturated states are compared with calculations based on a simple rate equation model at different heating rates. The experimental heating rates are included in these calculations. The symbols represent experiments and the lines TMAP7 simulations. The measured total retained D areal densities for each experiment are given in brackets.

sample. The first assumption is arguable, because the peak temperature is in a region where diffusion, although quite fast, might have an influence on the measured desorption rate by superposition of the release processes from states (1) and (2). The measured temperature ramp of the TPD experiment is considered in the calculation of the release rate, allowing more accurate comparisons but introducing noise to the simulation. A manual adjustment of the release rates

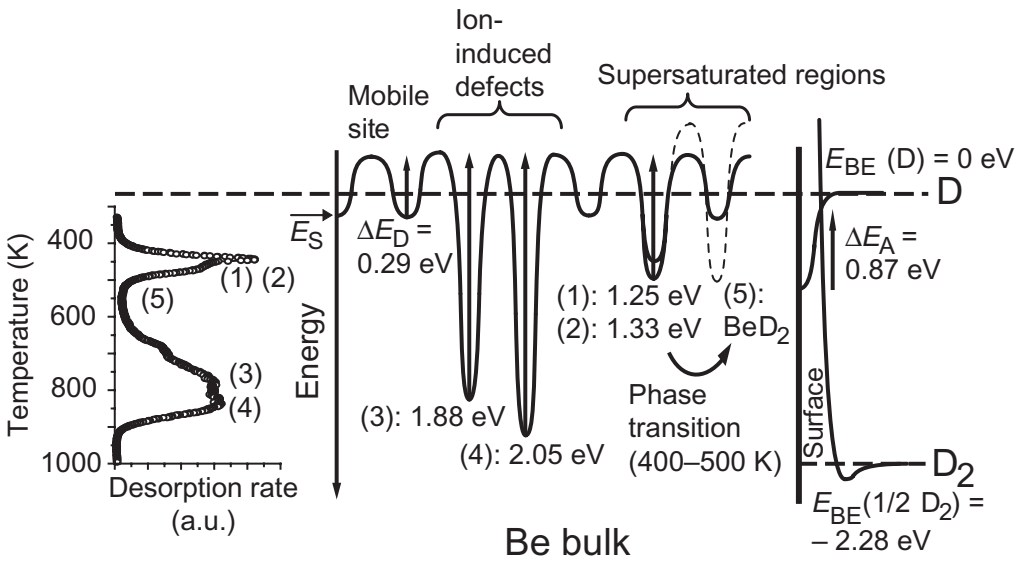

Figure 9. Schematic energy diagram (not to scale) illustrates the activation energies obtained from TPD experiments and calculations. Reference energy is free atomic D (= 0 eV). On the left side, a TPD spectrum shows the temperature dependence of the release from the binding states (1)–(5) for comparison with the determined activation energies. Surface desorption processes are illustrated on the right side.

of the model to the TPD experiments in the spectrum regions between 400 and 500 K yields activation energies of 1.25 and 1.33 eV for states (1) and (2), respectively. Different amounts N and heating rates $\partial T/\partial t$ result in good agreement between simulated and experimental rates as shown in figure 8(b). Nevertheless, the simulated release peaks are slightly broader than the experimental results, independent of the fit parameters E_A and the reaction order r. Inclusion of diffusive processes broadens the peaks even more. However, a frequency factor of $10^{20}\,s^{-1}$ calculates a spectrum with a peak width that gives better agreement with the experimental data (not shown). Such a high-frequency factor is physically unrealistic, as ν is usually related to the attempt frequency of a process. For this case, ν relates to the thermal vibration of a deuterium atom in the bulk. This indicates that the assumptions used in this model might be reasonable but incomplete. The release of deuterium from the supersaturated zone is not sufficiently described by a mere thermally activated process, but can additionally be influenced by the high D concentration and forces in the destabilized regions. This agrees with the qualitative picture drawn above on the nature of release states (1) and (2).

Based on the determined activation energies for the release processes from the various binding states of deuterium in Be, a schematic energy diagram is drawn in figure 9 (not to scale). Reference energy of a free D is set to 0 eV (upper horizontal line). The second reference energy is the binding energy of D in molecular form (D_2), which corresponds to an energy of −2.28 eV per D atom. Within the Be bulk, the activation energy for diffusion ($\Delta E_D = 0.29$ eV) represents the height of the energy barrier between two mobile sites, i.e., movement of D through the undisturbed Be lattice. The binding energy of D in a mobile (= solute) site is given by the dissolution energy E_S. Several values for E_S are given in the literature and vary between

0.1 eV [7, 29] and 1 eV [30]. According to this picture, the activation energy for the release of D bound in ion-induced trap sites (3) and (4) is the difference between its binding energy and $E_S + \Delta E_D$. Qualitatively, the activation energies for the different rate-limiting steps correspond to the peaks observed in a TPD spectrum (shown on the left side of figure 9). With increasing fluence, all available ion-induced trap sites (3) and (4) are saturated, such that the bulk lattice becomes locally supersaturated upon further D implantation. States (1) and (2) are created and lead to activation energies for the deuterium release of 1.25 and 1.33 eV, respectively. Elevated substrate temperatures (above RT, but below 570 K) can initiate a phase transition of the supersaturated areas into BeD_2, which decomposes at 570 K. The activation energy for $2D \rightarrow D_2$ recombination is $\Delta E_A = 0.87$ eV [18], leading to a desorption temperature similar to the release temperatures of state (1) or (2). However, as stated above, this recombination step is not a rate-limiting energy barrier for the release of implanted deuterium.

3.3.2. Modelling of retention by DFT. The models discussed above allow only indirect conclusions about the retention mechanism itself. A direct experimental characterization of the situation right after implantation is not possible by means of thermally activated release, as only activation energies for these processes and not the actual binding states and binding energies are accessible. First-principle calculations based upon spinpolarized gradientcorrected DFT can provide these insights [31, 32]. The link between activation energies for the various release processes and actual binding energies is illustrated in figure 9. Given a dissolution energy of $E_S = -0.1$ eV [7] (as assumed in figure 9), the binding energy of a D atom bound in a state corresponding to the release peak (i) would be $|E_{BE(i)}| = \Delta E_{A(i)} - \Delta E_D - E_S$. As an example for $i = 4$ one gets $\Delta E_{A(4)} = 1.86$ eV for the activation energy for the release from binding state (4). This binding energy can be compared with the interaction energy ΔE_{INT} of a single hydrogen atom with the rest of the calculation slab obtained from DFT. ΔE_{INT} is defined as $\Delta E_{INT} = E(m\mathrm{Be} + n\mathrm{H}) - E(m\mathrm{Be} - (n-1)\mathrm{H}) - E(\mathrm{H})$, where m is the number of Be atoms in the slab and n is the number of H atoms. The different hydrogen isotopes are considered to be identical. Energetically stable structures are obtained up to a ratio of $\mathrm{H/Be} \approx 3$. The average cohesive energy per atom of the system decreases linearly from $-2.7\,\mathrm{eV\,atom^{-1}}$ ($\mathrm{H/Be} = 1$) to $-1.5\,\mathrm{eV\,atom^{-1}}$ ($\mathrm{H/Be} = 3$). The minimum interaction energy of the single hydrogen atoms decreases from 1.7 eV at $\mathrm{H/Be} = 1$–0.2 eV at $\mathrm{H/Be} = 2.96$, corresponding to a decrease of the binding energy of hydrogen in the calculated structure. Within the structure, ΔE_{INT} exhibits variations of about 1 eV. However, such high interaction and thus binding energies suggest a smaller value for E_S in figure 9. For these calculations, the volume of the cell is kept constant. This would only approximate the real situation, where a certain swelling is observed in the AFM measurements in the form of protrusions, but on the other hand, free relaxation is inhibited by the surrounding material. Figure 10 illustrates the positions of the atoms (big spheres are Be, small ones hydrogen) in the cell with a ratio $\mathrm{H/Be} = 1$ and allowed volume expansion. The (originally) hexagonal Be lattice is dissolved. Nevertheless, this structure is energetically stable and gives a qualitative picture of the structure of the structural modifications in the supersaturated regions.

4. Summary

Based upon qualitative and quantitative evaluation of TPD spectra on clean and oxidized single crystalline Be, the retention mechanisms for implanted deuterium are identified. D is trapped in

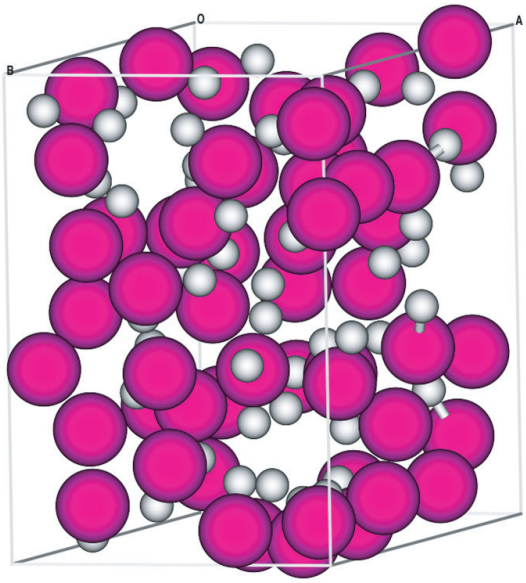

Figure 10. Calculated structure of a material with H/Be = 1 by DFT. The volume of the slab was allowed to expand. The original hexagonal Be lattice structure is dissolved by increasing the number of hydrogen atoms. This structure is energetically stable and gives an impression of the nature of the supersaturated regions created by ion implantation.

the Be bulk in defects created by the collision cascade and, at higher fluences, in destabilized (supersaturated) Be–D regions. A steady state is reached at a fluence of $2 \times 10^{17}\,\mathrm{cm}^{-2}$. An oxidized sample surface does not limit the thermally activated release rate. Provided there is enough thermal energy (implantation above RT), the supersaturated regions can transform into BeD_2, which starts to decompose above 500 K.

The investigations in this work provide for the first time experimental data for deuterium retention and thermal release of clean beryllium. It could be shown that the influence of surface oxide layers on the release of implanted deuterium is of minor importance. The experimental simplification of the investigated system with respect to surface and bulk chemistry (pure beryllium, pure monoenergetic deuterium implantation) and structure (single crystalline and annealed beryllium bulk) allows the thermal release to be modelled and thus leads to an understanding of the basic processes that govern deuterium retention.

The real Be first wall of ITER is different from the experimental conditions and sample structure in the experiments performed here. However, the results obtained here in well-defined single crystalline beryllium can be regarded as an upper limit for the expected retention of the real wall and allow a quantitative estimation. Lower deuterium energies or smaller angles of incidence to the surface will shift the implantation cascades towards the surface, leading to a shallower D profile and therefore a lower retained deuterium amount. For the case with the highest expected retention, such as areas where the wall is at low temperatures, so that all binding states can develop, a maximum amount of 7 g of hydrogen can accumulate in a (hypothetically) clean ITER Be wall with an area of $700\,\mathrm{m}^2$. This is also the upper limit for the contribution of the pure metallic main wall to the overall tritium inventory of ITER under the assumption of negligible isotope effects on the retention. Although thin BeO surface layers do

not influence retention in Be and release from Be itself, thicker BeO layers or other compound surface layers could still strongly influence the recycling behaviour. If hydrogen is implanted into these materials, their respective retention mechanisms could govern the recycling processes and require further investigations.

References

[1] Federici G *et al* 1998 *Fusion Eng. Des.* **39–40** 445
[2] Alimov V K, Chernikov V N and Zakharov A P 1997 *J. Nucl. Mater.* **241–3** 1047
[3] Doerner R P, Grossman A, Luckhardt S, Seraydarian R, Sze F C, Whyte D G and Conn R W 1998 *J. Nucl. Mater.* **257** 51
[4] Haasz A A and Davis J W 1997 *J. Nucl. Mater.* **241–3** 1076
[5] Wampler W R 1992 *J. Nucl. Mater.* **196–8** 981
[6] Won J, Doerner R P and Conn R W 1998 *J. Nucl. Mater.* **256** 96
[7] Anderl R A, Causey R A, Davis J W, Doerner R P, Federici G, Haasz A A, Longhurst G R, Wampler W R and Wilson K L 1999 *J. Nucl. Mater.* **273** 1
[8] Zalkind S, Polak M and Shamir N 1997 *Surf. Sci.* **385** 318
[9] Longhurst G 2004 INEEL/EXT-04–02352
[10] Reinelt M and Linsmeier C 2007 *Phys. Scr.* T **128** 111
[11] Alimov V K, Mayer M and Roth J 2005 *Nucl. Instrum. Methods Phys. Res.* B **234** 169
[12] Linsmeier C, Goldstrass P and Klages K U 2001 *Phys. Scr.* **T94** 28
[13] Roth J, Wampler W R and Jacob W 1997 *J. Nucl. Mater.* **250** 23
[14] Markin A V, Chernikov V N, Rybakov S Y and Zakharov A P 1996 *J. Nucl. Mater.* **233–7** 865
[15] Abramov E, Riehm M P, Thompson D A and Smeltzer W W 1990 *J. Nucl. Mater.* **175** 90
[16] Macaulay-Newcombe R G and Thompson D A 1994 *J. Nucl. Mater.* **212–5** 942
[17] Barabash V, Federici G, Linke J and Wu C H 2003 *J. Nucl. Mater.* **313–6** 42
[18] Lossev V and Küppers J 1993 *Surf. Sci.* **284** 175
[19] Wampler W R 1984 *J. Nucl. Mater.* **123** 1598
[20] Eckstein W 1991 *Computer Simulation of Ion–Solid Interactions* (Berlin: Springer)
[21] Eckstein W, Dohmen R, Mutzke A and Schneider R 2007 *IPP Report* 12/3
[22] Chernikov V N, Alimov V K, Markin A N and Zakharov A P 1996 *J. Nucl. Mater.* **228** 47
[23] Anderl R A, Hankins M R, Longhurst G R, Pawelko R J and Macaulay-Newcombe R G 1992 *J. Nucl. Mater.* **196–8** 986
[24] Barry P E, Bowers J S, Garza R G, Souers P C, Cantrell J S and Beiter T 1990 *J. Nucl. Mater.* **173** 142
[25] Baker R W, Brendel G J, Lowrance B R, Mangham J R, Marlett E M and Shepherd L H 1978 *J. Organomet. Chem.* **159** 123
[26] Maienschein J L, Bowers J S, Beiter T A and Cantrell J S 1993 *J. Alloys Compd.* **196** 1
[27] Ambrosek J A and Longhurst G R 2004 INEEL/EXT-04-01657
[28] de Jong A M and Niemantsverdriet J W 1990 *Surf. Sci.* **233** 355
[29] Shapovalov V I and Dukel'ski Y M 1984 *Russ. Metall.* **5** 210
[30] Swansiger W A 1986 *J. Vac. Sci. Technol.* A **4** 1216
[31] Allouche A 2008 *Phys. Rev.* B **78** 085429
[32] Allouche A and Linsmeier C 2008 *J. Phys.: Conf. Ser.* **117** 012002